state. In spite of these differences, the three structures show fairly similar modal properties.

ACKNOWLEDGMENTS

The authors wish to thank Prof. P. Khastgir for his keen interest in this work.

REFERENCES

1. J.E. Goell, A circular harmonic computer analysis of rectangular dielectric waveguides, Bell Syst Tech J 48 (1969), 2133–2160.
2. K.S. Chiang, Analysis of the effective index method for the vector modes rectangular-core dielectric waveguide, IEEE Trans Microwave Theory Tech 44 (1996), 692–700.
3. K.S. Chiang, Finite element method for cutoff frequencies of weakly guiding fibers of arbitrary cross-section, Opt Quantum Electron 16 (1984), 487–493.
4. S.R. Rangaranjan and J.E. Lewis, First higher-mode cutoff in two-layer elliptical fiber waveguides, Electron Lett 16 (1980), 263–264.
5. C. Yeh, Modes in weakly guiding elliptical optical fibers, Opt Quantum Electron 8 (1976), 43–47.
6. R.B. Dyott, Cutoff of the first order modes in elliptical dielectric waveguide: An experimental approach, Electron Lett 26 (1990), 1721–1723.
7. M.P. Srinivasa Rao, B. Prasad, P. Khastgir, and S.P. Ojha, Modal cutoff conditions for an optical waveguide with a hypocycloidal cross section, Microwave Opt Technol Lett 14 (1997), 177–180.
8. V. Singh, S.P. Ojha, B. Prasad, and L.K. Singh, Optical and microwave dispersion curves of an optical waveguide with a guiding region having a cross-section with a lunar shape, Optik 110 (1999), 267–270.
9. V. Singh, S.P. Ojha, and L.K. Singh, Modal behavior, cutoff condition, and dispersion characteristics of an optical waveguide with a core cross section bounded by two spirals, Microwave Opt Technol Lett 21 (1999), 121–124.
10. V. Singh, S.P. Ojha, and B. Prasad, Weak guidance modal dispersion characteristics of an optical waveguide having core with sinusoidally varying gear shaped cross section, Microwave Opt Technol Lett 22 (1999), 129–133.
11. V. Singh, B. Prasad, and S.P. Ojha, An analytical study of the cutoff conditions and the dispersion curves of a waveguide with a cross-sectional shape resembling an elipse compressed along the minor axis, Microwave Opt Technol Lett (1999).
12. V. Singh, B. Prasad, and S.P. Ojha, An analytical study of the modal characteristic and dispersion curves of an infrared-optical waveguide having a cross section with a four-lobed loop boundary, Microwave Opt Technol Lett (1999).
13. V. Singh, B. Prasad, and S.P. Ojha, Weak guidance dispersion characteristics of an infrared waveguide having cross-section with a three lobed loop boundary, Optik (1999).
14. V.N. Mishra, V. Singh, B. Prasad, and S.P. Ojha, An analytical investigation of dispersion characteristic of a lightguide with an annular core cross section bounded by two cardioids, Microwave Opt Technol Lett (1999).
15. M.P.S. Rao, V. Singh, B. Prasad, and S.P. Ojha, An analytical study of the dispersion curves of an annular waveguide mode of liquid crystal, Photon Optoelectron 5 (1998), 73–88.
16. B. Prasad, M.P.S. Rao, V. Singh, and S.P. Ojha, Modal characteristics and cutoff conditions of a hypocycloidal waveguide with chiral media in the core and the cladding, Optik (1999).
17. S.P. Ojha, P.K. Choudhury, and P. Khastgir, Glass fibers of triangular cross-section with metal loading on one or more sides: A comparative modal study, Proc SPIE 1580 (1991), 278–287.
18. P. Sharan, P. Khastgir, S.P. Ojha, and B. Prasad, Metal-clad optical waveguide with a cardioid shaped cross-section and their modal characteristics, Microwave Opt Technol Lett 16 (1997), 271–275.
19. M.P.S. Rao, V. Singh, B. Prasad, P. Khastgur, and S.P. Ojha, Modal cutoff conditions of a hypocycloidal waveguide with various types of metal loading on the core boundaries, Microwave Opt Technol Lett 19 (1998), 152–158.
20. V. Singh, B. Prasad, and S.P. Ojha, Modal dispersion characteristics of a metal-clad optical waveguide with a guiding cross-section resembling a lune, Photon Optoelectron (1999).
21. V.N. Mishra, V. Singh, B. Prasad, and S.P. Ojha, Weak guidance modal dispersion curves of an optical waveguide having a double convex lens cross section, Microwave Opt Technol Lett (1999).

CCC 0895-2477/00

ASYMPTOTIC WAVEFORM EVALUATION FOR SCATTERING BY A DISPERSIVE DIELECTRIC OBJECT

Dan Jiao[1] and Jian-Ming Jin[1]
[1] Center for Computational Electromagnetics
Department of Electrical and Computer Engineering
University of Illinois
Urbana, Illinois 61801-2991

Received 18 August 1999

ABSTRACT: *The asymptotic waveform evaluation (AWE) method is applied to the moment-method solution of scattering by a dispersive dielectric object, resulting in an efficient technique for the calculation of the radar cross section over a specified frequency band.* © 2000 John Wiley & Sons, Inc. Microwave Opt Technol Lett 24: 232–234, 2000.

Key words: *asymptotic waveform evaluation; electromagnetic scattering; moment method*

1. INTRODUCTION

A formulation that is widely used for scattering by a dielectric object is the so-called PMCHW [1], named after Poggio, Miller, Chang, Harrington, and Wu, who originally developed the formulation. In this formulation, the electric-field integral equation (EFIE) for the field inside the dielectric object is combined with the EFIE for the field outside the object to form a combined equation. Similarly, the magnetic-field integral equation (MFIE) for the field inside the object is combined with the MFIE for the field outside the object to form another combined equation. These two equations are then solved by the moment method. This formulation is found to be free of interior resonances, and yields accurate and stable solutions. This letter describes the application of the asymptotic waveform evaluation (AWE) method [2] to the PMCHW-based moment method to accelerate the calculation of the scattering by a dispersive dielectric object, whose permittivity is characterized by the Debye model.

2. FORMULATION

Consider an arbitrarily shaped homogeneous dielectric scatterer characterized by permittivity ϵ_2 and permeability μ_2, and immersed in an infinite and homogeneous medium having permittivity ϵ_1 and permeability μ_1. Using either the equivalence principle or the vector Green's theorem, one can formulate a set of four integral equations to calculate the electric and magnetic fields $\mathbf{E}$ and $\mathbf{H}$ in terms of equivalent electric and magnetic currents $\mathbf{J}$ and $\mathbf{M}$ on the surface of the scatterer. The equation to calculate the electric field is known as the EFIE, and there are two such equations: one is for the field inside the object (EFIE-I), and the other is for the field outside the object (EFIE-O). The equation to calculate the magnetic field is known as the MFIE, and there are also two such equations: one is for the field inside the object (MFIE-I), and the other is for the field outside the object (MFIE-O). A simple combination of EFIE-I and EFIE-O yields an integral equation:

$$[Z_1\mathbf{L}_1(\mathbf{J}) + Z_2\mathbf{L}_2(\mathbf{J}) - \mathbf{K}_1(\mathbf{M}) - \mathbf{K}_2(\mathbf{M}) = \mathbf{E}^i]_{\tan} \quad (1)$$

and a similar combination of MFIE-I and MFIE-O results in another integral equation:

$$[Z_1\mathbf{K}_1(\mathbf{J}) + Z_2\mathbf{K}_2(\mathbf{J}) + \mathbf{L}_1(\mathbf{M}) + \mathbf{L}_2(\mathbf{M}) = Z_1\mathbf{H}^i]_{\tan} \quad (2)$$

where $Z_i = \sqrt{\mu_i/\epsilon_i}$, and $\mathbf{L}_i$ and $\mathbf{M}_i$ are integral operators defined by

$$\mathbf{L}_i(\mathbf{X}) = jk_i \int_S \left[\mathbf{X}(\mathbf{r}') + \frac{1}{k_i^2}\nabla\nabla'\cdot\mathbf{X}(\mathbf{r}')\right] G_i(\mathbf{r},\mathbf{r}')\, dS' \quad (3)$$

$$\mathbf{K}_i(\mathbf{X}) = \int_S \mathbf{X}(\mathbf{r}') \times \nabla G_i(\mathbf{r},\mathbf{r}')\, dS' \quad (4)$$

in which $k_i = \omega\sqrt{\mu_i\epsilon_i}$, S denotes the surface of the scatterer, and $G_i(\mathbf{r},\mathbf{r}')$ is the scalar Green's function given by

$$G_i(\mathbf{r},\mathbf{r}') = \frac{e^{-jk_i|\mathbf{r}-\mathbf{r}'|}}{4\pi|\mathbf{r}-\mathbf{r}'|}. \quad (5)$$

Equations (1) and (2) are known as the PMCHW formulation [1]. When $\mathbf{r} = \mathbf{r}'$, the integral in (4) is interpreted in the principal value sense.

For a dispersive dielectric object, ϵ_2 and μ_2 can be a function of frequency. For simplicity, we assume that μ_2 is a constant, and only ϵ_2 varies with frequency. The complex permittivity of a dielectric can be described by the Debye model [3]:

$$\epsilon_2(\omega) = \epsilon_2'(\omega) - j\epsilon_2''(\omega) = \epsilon_{2\infty}' + \frac{\epsilon_{2s}' - \epsilon_{2\infty}'}{1 + j\omega\tau_e} \quad (6)$$

where ϵ_{2s}' denotes the static dielectric constant, $\epsilon_{2\infty}'$ is the optical dielectric constant, and τ_e is a relaxation time constant related to the original relaxation time constant τ by

$$\tau_e = \tau\frac{\epsilon_{2s}' + 2\epsilon_0}{\epsilon_{2\infty}' + 2\epsilon_0} \quad (7)$$

with ϵ_0 denoting the permittivity of free space.

Equations (1) and (2) can be solved numerically using the moment method. In this work, the Rao–Wilton–Glisson function [4] is used both as an expansion and testing function. The solution is shown to be accurate and stable at interior resonances [5]. The resulting matrix equation can be symbolically written as

$$A(\omega)x(\omega) = y(\omega) \quad (8)$$

where A is a square matrix, x is an unknown vector consisting of the discretized equivalent electric and magnetic currents, and y is a known vector associated with the incident electric and magnetic fields $(\mathbf{E}^i, \mathbf{H}^i)$. Since the matrix A depends on frequency, it must be generated and solved repeatedly at each frequency in order to obtain a solution over a frequency band, which can be time consuming.

To accelerate the solution of (8) over a frequency band, we employ the AWE method. In accordance with this method [2], $x(\omega)$ is expanded into a rational function:

$$x(\omega) = \frac{\sum_{i=0}^{L} a_i(\omega - \omega_0)^i}{1 + \sum_{j=1}^{M} b_j(\omega - \omega_0)^j} \quad (9)$$

where ω_0 denotes the expansion point. The expansion coefficients a_i and b_j can be determined from the inverse and the $L + M$ derivatives of A and the $L + M$ derivatives of y at frequency ω_0. In the case where one expansion point is not

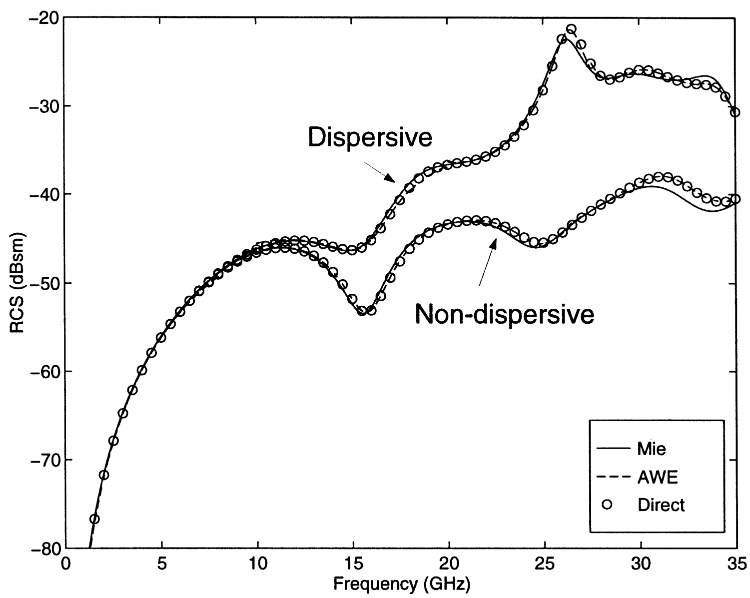

Figure 1 Backscatter RCS versus frequency of a dielectric sphere having a radius of 0.5 cm

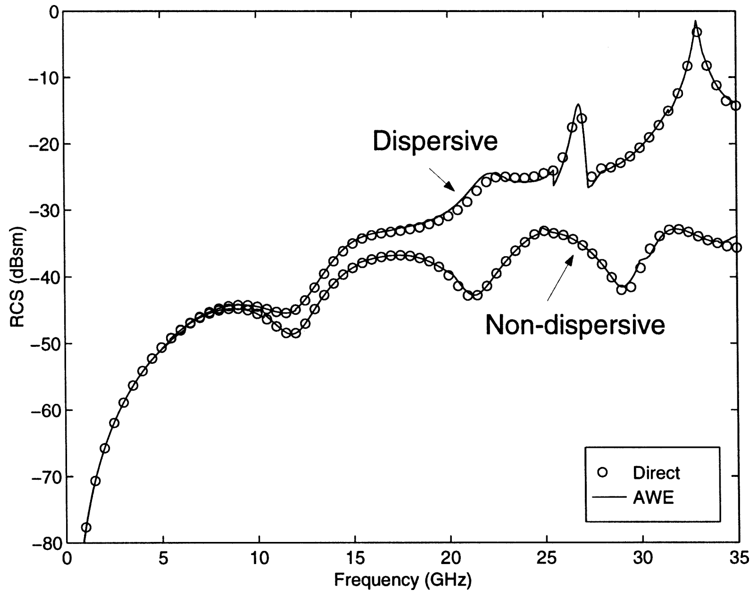

Figure 2 Backscatter RCS versus frequency of a dielectric cube having a side length of 1 cm

sufficient to cover the desired frequency band, one can use multipole expansion points, which can be selected automatically using a simple binary search algorithm [6].

3. NUMERICAL EXAMPLES

Consider a dielectric sphere of radius 0.5 cm immersed in free space. For the numerical solution, the surface of the sphere is modeled by 648 triangular patches, resulting in 972 edges, and thus 1944 unknowns. The permittivity of the sphere is characterized by $\epsilon'_{rs} = 2.56$, $\epsilon'_{r\infty} = 1.0$, and $\tau = 1.59$ ps/rad. As a result, as the frequency varies from 0.5 to 35 GHz, the real part of the relative permittivity varies from 2.56 to 2.22, and the imaginary part varies from -0.012 to -0.65. The backscatter radar cross section (RCS) of the sphere is shown in Figure 1, where the backscatter RCS of a nondispersive sphere of the same size and having a relative permittivity 2.56 is also given. Three solutions are displayed in the figure. One is the exact Mie series solution, the second is the solution obtained by solving (8) directly at each frequency, and the third is the solution obtained using the AWE method. With a frequency step of 0.5 GHz, it takes the direct method 24611 s to obtain the solution on a digital personal workstation (500 MHz Alpha 21164 processor). In contrast, the AWE method produces the solution with 0.01 GHz increments in 2206 s on the same computer. Figure 2 shows similar results for a 1 cm × 1 cm × 1 cm dielectric cube with normal incidence.

4. CONCLUSIONS

This letter described the application of the AWE method to the moment-method solution of the PMCHW equations for scattering by a dispersive dielectric object. It was shown that the use of AWE can speed up the calculation by more than an order of magnitude.

REFERENCES

1. J.R. Mautz and R.F. Harrington, Electromagnetic scattering from a homogeneous material body of revolution, AEU 33 (1979), 71–80.
2. L.T. Pillage and R.A. Rohrer, Asymptotic waveform evaluation for timing analysis, IEEE Trans Computer-Aided Design 9 (1990), 352–366.
3. A.R. von Hippel, Dielectrics and waves, M.I.T. Press, Cambridge, MA, 1954.
4. S.M. Rao, D.R. Wilton, and A.W. Glisson, Electromagnetic scattering by surfaces of arbitrary shape, IEEE Trans Antennas Propagat AP-30 (1982), 409–418.
5. X.Q. Sheng, J.M. Jin, J. Song, W.C. Chew, and C.C. Lu, Solution of combined-field integral equation using multilevel fast multipole algorithm for scattering by homogeneous bodies, IEEE Trans Antennas Propagat 46 (1998), 1718–1726.
6. M.A. Kolbehdari, M. Srinivasan, M.S. Nakhla, Q.J. Zhang, and R. Achar, Simultaneous time and frequency domain solutions of EM problems using finite element and CFH techniques, IEEE Trans Microwave Theory Tech 44 (1996), 1526–1534.

CCC 0895-2477/00

SLOT-LOADED RECTANGULAR MICROSTRIP ANTENNA FOR DUAL-FREQUENCY OPERATION

Jui-Han Lu[1]
[1] Department of Electronic Communication Engineering
National Kaohsiung Institute of Marine Technology
Kaohsiung, Taiwan 811, R.O.C.

Received 24 August 1999

ABSTRACT: *A new design of a slot-loaded rectangular microstrip antenna for single-feed dual-frequency operation is proposed and experimentally studied. The slots loaded in the patch are a pair of bent slots centered in the patch and oriented along the resonant direction, with the spacing between the two slots being about half the patch's radiating-edge length. By varying the bent angle and horizontal-section length of the slots, the frequency ratio between the two operating frequencies is tunable in a range from about 1.28 to 1.79. The two frequencies are also of the same polarization planes and similar broadside radiation patterns.*
© 2000 John Wiley & Sons, Inc. Microwave Opt Technol Lett 24: 234–237, 2000.